Micromolar Concentration Affinity Study on a Benchtop NMR Spectrometer with Secondary 13C Labeled Hyperpolarized Ligands

Author(s):
Cala, Olivier; Bocquelet, Charlotte; Gioiosa, Chloé; Torres, Felix; Cousin, Samuel F.; Guibert, Sylvie; Ceillier, Morgan; Busse, Venita; Decker, Frank; Kempf, James G.; Elliott, Stuart J.; Stern, Quentin; Bornet, Aurélien; Jannin, Sami

Publication date:
2025-02-04

Permanent link:
https://doi.org/10.3929/ethz-b-000720401

Originally published in:
ACS Omega 10(4), https://doi.org/10.1021/acsomega.4c05101

ACS OMEGA

Open Access

http://pubs.acs.org/journal/acsodf

Article

Micromolar Concentration Affinity Study on a Benchtop NMR Spectrometer with Secondary ^{13}C Labeled Hyperpolarized Ligands

Olivier Cala, Charlotte Bocquelet, Chloé Gioiosa, Felix Torres, Samuel F. Cousin, Sylvie Guibert, Morgan Ceillier, Venita Busse, Frank Decker, James G. Kempf, Stuart J. Elliott, Quentin Stern, Aurélien Bornet, and Sami Jannin*

Cite This: *ACS Omega* 2025, 10, 3332−3337

Read Online

ACCESS | Metrics & More | Article Recommendations | Supporting Information

ABSTRACT: Benchtop NMR is becoming an increasingly important tool, sometimes providing a simple and low-cost alternative to high-field NMR. The Achilles heel of NMR and even more critically of benchtop NMR is its limited sensitivity. However, when combined with hyperpolarization techniques, the sensitivity boost can provide excellent sensitivity that can even make benchtop NMR compatible with affinity studies for drug discovery. Hyperpolarization by dissolution dynamic nuclear polarization (dDNP) provides a route to enhancing ^{13}C nuclear magnetic resonance (NMR) sensitivity by more than 5 orders of magnitude for a wide range of small molecules on a benchtop NMR system. We show here how ligands can be secondarily labeled with ^{13}C tags and hyperpolarized with conventional dDNP methods. These hyperpolarized ligands display long nuclear spin−lattice relaxation time constants and can therefore be used to probe interactions with target proteins in conventional dDNP settings. The boost in sensitivity combined with the simplicity of the ^{13}C spectra (one peak per ligand) enables detection on an 80 MHz benchtop NMR spectrometer at micromolar concentrations, which may ultimately provide a way of improving and accelerating the discovery of new drug candidates.

Benchtop NMR micromolar affinity studies with hyperpolarized ligands

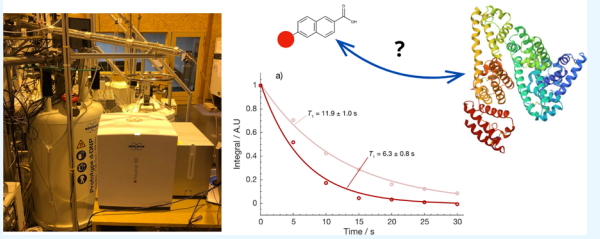

INTRODUCTION

Identifying intermolecular interactions is at the core of life science, from biological mechanisms in living organisms to the interaction between biomolecules and exogenous molecules, such as drugs. In drug discovery, identifying protein−ligand interactions is a crucial step in the further design of more potent and specific ligands to achieve drug candidates. This identification step is called screening, as several thousands of molecules are tested to identify which interact with a target biomolecule, often a protein. Screening requires a sufficient throughput to test these libraries, and it must be accurate to deliver high-quality primary data sets that will be leveraged by medicinal chemists for drug design. The ideal screening method should be fast and require a low sample production and preparation effort. In the past 20 years, fragment-based drug design (FBDD) has been established as a valid strategy to tackle challenging biomolecular targets.[1] FBDD requires screening methods that can detect the weakly interacting hits that are mostly achieved with fragments. These initial hits consisting of fragments are later assembled through fragment merging, linking, or growing to form higher affinity (typically μM) ligands.[2,3]

Nuclear magnetic resonance (NMR) has emerged over the past decades as a powerful method for screening, providing full protein−ligand characterizations, particularly for weakly interacting systems,[4] in complement to other techniques.[5−9] Due to its high robustness, NMR is the gold standard used in pharmaceutical research to identify and validate hits from compound libraries in drug discovery.

NMR screening experiments can be classified into two families: protein-observed experiments or ligand-observed experiments.[8,10] Protein-observed experiments often require $^{13}C/^{15}N$ labeling, which is not always feasible for large proteins (mass exceeding 30 kDa with intense relaxation). The classical ligand-observed ^{1}H NMR methods [saturation transfer difference (STD), water-ligand observed through gradient spectroscopy (waterLOGSY), nuclear Overhauser spectroscopy (NOESY), and relaxation-based methods] do not require isotopic labeling of the protein but do require ligand concentrations on the order of hundreds of micromolar (typically for a 20 min experiment). Such NMR screening is systematically performed on high-field NMR spectrometers ($\omega_0/2\pi$ > 500 MHz) and remains incompatible with low-field

Received: May 30, 2024
Revised: January 10, 2025
Accepted: January 17, 2025
Published: January 24, 2025

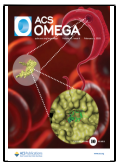

benchtop NMR because of a lack of sensitivity. One efficient approach is to involve hyperpolarization methods, yielding out-of-Boltzmann polarization and enhanced sensitivity.

Dissolution dynamic nuclear polarization (dDNP)[11] is a hyperpolarization method that can boost NMR sensitivity up to 5 orders of magnitude in the context of benchtop NMR. It was successfully used in interaction studies, for example, by Hilty et al.[12] using hyperpolarized fluorine-containing molecules, by Lerche et al.[13] using natural abundance ^{13}C molecules and relaxation-based methods, by Kurzbach et al.[14] by exploring hyperpolarized long-lived state relaxation in deuterated methyl groups, or by Jannin et al.[15] using a waterLOGSY experiment combined with hyperpolarized water to reveal weak binding. Although successful and promising, these approaches still suffer from some critical limitations: (i) ^{1}H and ^{19}F have short nuclear spin−lattice relaxation time constants (T_1) on the order of a second, meaning that hyperpolarization is short-lived and that the large enhancement brought by dDNP rapidly vanishes; (ii) ^{13}C nuclear spins have longer values of T_1, which make them much more interesting candidates, but the natural abundance of only 1.1% translates into a suboptimal sensitivity, and the very long hyperpolarization time (up to 3 h to hyperpolarize a single sample) translates into a very low throughput; and (iii) all presented methods were limited to weak affinity.

In the past decade, Raftery and co-workers presented the chemical derivatization of amines in biofluids with [1,1′-$^{13}C_2$] acetic anhydride.[16] This easy and robust reaction takes place rapidly using [1,1′-$^{13}C_2$] acetic anhydride in an aqueous solution at ambient temperature on the amine.

Here, we propose to revisit this secondary labeling approach in the context of NMR drug screening by exploiting a chemical derivation of NH_2-containing molecules to develop a new ^{13}C-labeled ligand library that is chemically distinct and with different binding properties and couple it with our most recent $^{1}H \rightarrow {}^{13}C$ cross-polarization (CP)-assisted approaches leading to high (>30%) and fast (10 min) ^{13}C hyperpolarization. Similar to Torres et.al.,[17] we restrict for now our chemical space to NH_2-containing molecules, thus limiting the possible chemical diversity. However, this approach could be generalized to many more molecules later by competition binding experiments or by ^{13}C enrichment. We used hyperpolarized ^{13}C-based relaxation studies at a few micromolar ligand concentrations against a model protein on an 80 MHz benchtop NMR spectrometer. We show that despite the inherent low sensitivity of the system and its limited resolution, and thanks to the high hyperpolarization brought by dDNP and the simplicity of the resulting ^{13}C spectra (one peak per ligand), our method enables the detection and identification of ligands at a few μM concentration within seconds after 20 min of hyperpolarization.

RESULTS AND DISCUSSION

Figure 1a illustrates the chemical reaction used to tag NH_2-containing molecules. When acetic anhydride is added in aqueous solution at room temperature, NH_2-containing molecules derivatize rapidly. Here, 6-amino-2-naphthoic acid and glycine were used as test molecules. The N-acetylation occurs on the primary amine group simply by adding an excess of acetic anhydride at room temperature, with a yield greater than 95%. The new products are N-Acetyl [1-^{13}C]-6 amino-2-naphthoic acid and N-Acetyl [1-^{13}C]-glycine, here named Ac-L30 and Ac-L08, respectively. Their ^{13}C assignments are

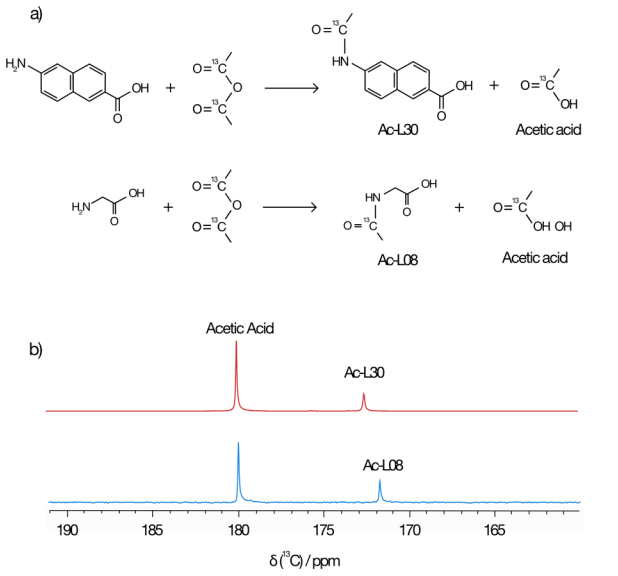

Figure 1. (a) Chemical reaction for the labeling of a ligand containing an -NH_2 group as described in the experimental section. (b) Relevant portions of the experimental ^{13}C NMR spectra for the 164 mM tagged ligand of N-Acetyl [1-^{13}C]-6-amino-2-naphthoic acid (N−Ac-L30, red) and N-Acetyl [1-^{13}C]-glycine (Ac-L08, blue) dissolved in a deuterated phosphate buffer and acquired at 20 MHz (1.88 T) and 298 K.

shown in Figure 1b. The ^{13}C NMR spectra of the N-acetylated derivatives show the presence of the isotopically labeled carbonyl sites that appear in the 173−182 ppm region. It can be seen that the individual N-acetyl-molecules are well resolved with a single peak for each molecule with a full-width half-maximum (fwhm) < 1 Hz at 171.75 ppm for Ac-L30 and at 172.55 ppm for Ac-L08. An additional peak is observed at 180 ppm corresponding to [1-^{13}C] acetic acid (resulting from the excess of anhydride acetic acid during synthesis). The derivatization procedure results in a direct ^{13}C NMR sensitivity gain of 91 with respect to a nonlabeled molecule. Any primary amine group containing molecule can be labeled with the presented approach, which results in a new molecule that can be used as a candidate for interaction tests. These compounds containing a ^{13}C center by ^{13}C acetylation of amines evidently become chemically distinct and have different binding properties. These new compounds have been tested with conventional approaches, i.e., STD and ^{13}C T_1 relaxation measurements.

For the current study, HSA was used as a model protein target. Figure 2 shows the result of a conventional STD interaction test with the HSA protein measured at 600 MHz. We see that Ac-L30 (^{1}H 1D reference spectrum (b) in black and STD spectrum (a) in red) interacts with HSA with a strong STD signal (dashed area), whereas Ac-L08 (^{1}H 1D reference spectrum (d) in black and STD spectrum (c) in blue) has a much lower STD signal translating into an insignificant interaction with HSA.

Figure 3 shows the ^{13}C signal decays of hyperpolarized ligands measured at 600 μM concentration after hyperpolarization and injection, with and without the HSA protein at 40 μM concentration. T_1 measurements were acquired on an 80 MHz benchtop NMR spectrometer after hyperpolarization with our previously developed dDNP methodology,[18] including low-temperature DNP and $^{1}H \rightarrow {}^{13}C$ cross-

https://doi.org/10.1021/acsomega.4c05101
ACS Omega 2025, 10, 3332−3337

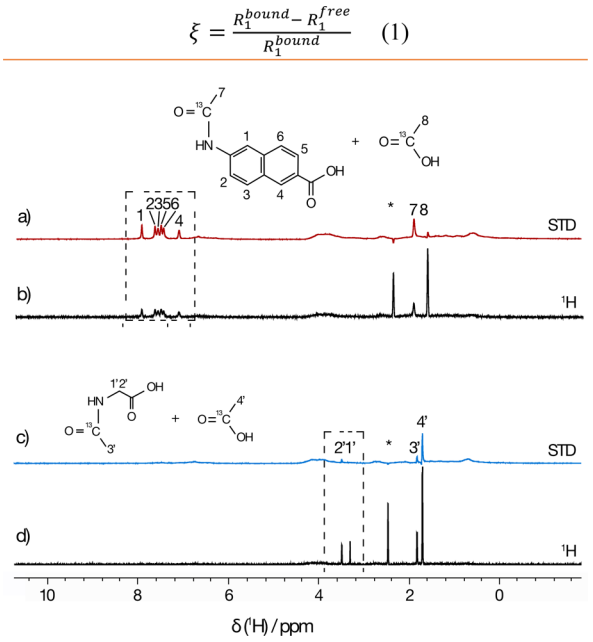

Figure 2. Relevant portions of the experimental STD and ^{1}H NMR spectra of 2 mM Ac-L08 with 5 μM HSA in 0.5% DMSO-d_6, 10% D_2O, and 89.5% phosphate buffer pH 8.5 (v:v:v) (a, b) and 2 mM Ac-L30 with 5 μM HSA in 0.5% DMSO-d_6, 10% D_2O, and 89.5% phosphate buffer pH 8.5 (v:v:v) (c, d) acquired at 600 MHz (14.1 T) and 298 K with 16 and 512 scans, respectively. Assignments are indicated for the two compounds (1′-4′ for Ac-L08 and 1−8 for Ac-L30). * indicates the signal corresponding to DMSO-d_6. The dashed boxes represent the area of interest for the STD signal.

polarization,[19−22] fast dissolution and transfer[23] through a magnetic tunnel,[24] and injection (see Methods section for experimental details). These standardized methods were previously applied in the field of metabolomics[25−27] and will soon be part of a commercial polarizer. Note that using hyperpolarized T_1 variation as a probe for interactions entirely lifts the issue of repeatability in the initial polarization. Here, we observe notable changes in ^{13}C T_1's caused by ligand-protein interactions. This is not surprising and confirms that the study is designed appropriately and that our method works straightforwardly. Without protein, we measured ^{13}C T_1 values of 11.9 ± 1.0 s for Ac-L30 and 29.3 ± 0.2 s for Ac-L08. When HSA was present in the NMR tube before ligand injection and mixed during injection, we observed a drop in ^{13}C T_1 for Ac-L30 down to 6.3 ± 0.8 s, while the ^{13}C T_1 of the noninteracting control, Ac-L08, was not significantly affected. The contrast (ξ) in ^{13}C $R_1 = 1/T_1$ can be defined as the difference between ^{13}C R_1 without (free) and with protein (bound), normalized by ^{13}C R_1 with protein:

$$\xi = \frac{R_1^{\text{bound}} - R_1^{\text{free}}}{R_1^{\text{bound}}} \quad (1)$$

ξ was found to be 1.40 ± 0.02% for the noninteracting Ac-L08 and 47 ± 8% for Ac-L30. These results qualitatively agree with thermal equilibrium experiments shown in Supporting Information. Note that, for sensitivity reasons, these thermal equilibrium experiments were performed with excessively high concentrations of ligands (164 mM instead of 600 μM, thus 273 times higher) and with 1 mM HSA. While these control experiments took 8.5 h at 1.88 T with 164 mM ligands, they

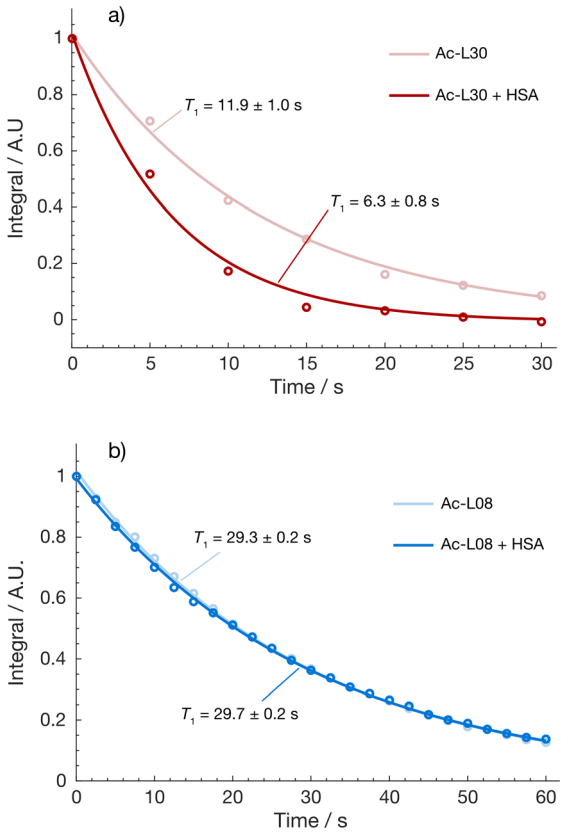

Figure 3. Experimental decays for the hyperpolarized ^{13}C NMR signal of 600 μM Ac-L30 and 600 μM Ac-L08 dissolved in deuterated-phosphate buffer pH 8.5 acquired at a 20 MHz ^{13}C frequency (1.88 T) and ∼303 K with and without mixing with a protein solution (40 μM HSA) after 2 s transfer to the NMR spectrometer. (a) ^{13}C T_1 determination for Ac-L30 without and with HSA. (b) ^{13}C T_1 determination for Ac-L08 without and with HSA. For both ligands, hollow circles represent experimental data (integrals of 1D ^{13}C NMR spectra measured with 5 or 2.5 s intervals and pulse flip angles of 15°), and the solid lines represent fits of the experimental data with a monoexponential decay function: $P_0 \cdot \exp(-t/T_1)$ where P_0 is a fitting constant.

would have taken 273^2more time, equivalent to more than 72 years, with 600 μM ligands and without hyperpolarization at 1.88 T, instead of about 1 h with hyperpolarization. Finally, these results show that our hyperpolarization and dissolution procedure does not influence the sample health and longitudinal relaxation time constants and therefore yields useful interaction information (Ac-L08 interacts significantly less than Ac-L30 with the protein). This demonstrates both efficient labeling of NH_2-containing molecules and possible interaction studies based on the ^{13}C T_1 decay measurement following hyperpolarization by state-of-the-art CP-assisted dDNP methods. We were able to hyperpolarize these compounds and use their ^{13}C T_1 values as a probe of protein−ligand interaction with increased sensitivity at concentrations down to 30 μM with a signal-to-noise ratio (SNR) exceeding 100, even on a benchtop NMR spectrometer operating at 1.88 T. Extra orders of magnitude in sensitivity could evidently be afforded on high field spectrometers if needed.

This method can potentially bring significant benefits in terms of throughput. Furthermore, if we consider the work of previous groups[16,28,29] where up to 20 labeled amino acids

https://doi.org/10.1021/acsomega.4c05101
ACS Omega 2025, 10, 3332−3337

were mixed, we speculate that such an approach could be extended to the study of more than 30 mixed ligands simultaneously screened in one shot (as sometimes done for ^{19}F, while for ^{1}H, it is classically only 5−10 ligands[30,31] that are mixed due to ^{1}H NMR signal superposition). Hyperpolarizing such ligand mixtures can typically be repeated every 30 min to an hour depending on the skills of the operator of the dDNP setup. Further automation in the future might bring this number down to 10−20 min, which would translate into two to four thousand ligands potentially screened per day.

The described screening method benefits from the dramatically enhanced ^{13}C NMR signal intensity engendered by implementing hyperpolarization methodologies, in this case, dDNP, leading to reduced protein and ligand concentrations in the μM range. These concentrations may open the way to targeting proteins that are difficult to express or poorly soluble and ligands that have higher affinities and therefore need to be at concentrations close to the protein.

Here, NH_2-containing molecules are tagged in a way that applies to hundreds of molecules in our library. Other tags or chemical labeling schemes and the ^{13}C-enrichment of ligands could be envisaged, in particular, for competition experiments with a known ligand. Furthermore, the recent developments in isotope swap will open the way to a further growing number of specifically ^{13}C-labeled small molecules at affordable costs,[32] and other carbon insertion methods are expandable to ^{13}C insertion from economical precursors[33] to provide sufficient diversity in fragment libraries. The small molecule selective labeling approach can also be expanded to other nuclear spins, such as ^{15}N, which also benefits from long spin−lattice relaxation time constants, a comprehensive chemical shift range, and CP-assisted dDNP methodologies developed in our laboratories.[34] Recently, the insertion of ^{15}N atoms into diverse aromatic skeletons has demonstrated the possibility of generating chemically diverse scaffolds containing single ^{15}N atoms.[35−37] Finally, here, we measured T_1 as a contrast parameter to detect the binding; however, extending the method to measurements of transverse relaxation might yield an even higher contrast.

CONCLUSIONS

In conclusion, we have shown that NH_2-containing ligands can be labeled efficiently and that their interactions with the HSA protein can be measured by either classical ^{1}H NMR approaches (such as STD) or hyperpolarized ^{13}C T_1 contrast. We were able to hyperpolarize these compounds and measure their T_1 values with sufficient sensitivity at concentrations down to 30 μM in a benchtop NMR spectrometer operating at an 80 MHz frequency for protons, which provided evidence of binding in a single experiment. The method might be extended in the future to the simultaneous study of many ligands mixed and screened in one shot, as ^{13}C NMR spectra are simple (one peak per ligand) and better resolved than conventional ^{1}H spectra. The required sample concentrations are compatible with targeting proteins that are difficult to express or poorly soluble and ligands that have higher affinity and are potentially better drug candidates. This approach might have the potential to become a useful screening method, in particular, in the context of FBDD. In the future, we plan on applying this method to a larger library of ligands and extending it to competitive studies either by using the tag approach or by directly incorporating a ^{13}C label into known ligands.

METHODS

Chemicals. All chemicals were purchased from Sigma-Aldrich.

Labeling. For the derivatization of ligands, stock solutions of 2 commercial molecules (200 mM glycine and 6-amino-2-naphthoic acid in 400 mM deuterated phosphate buffer (pH 8.5) and DMSO, respectively) were prepared in separate tubes. For the derivatization of individual molecules, 250 μL of each compound was reacted 5 times with 1 μL of 1,1′-$^{13}C_2$ acetic anhydride and 10 μL of NaOD 1 M at room temperature, producing 305 μL at 164 mM of each labeled molecule.

DNP Sample Preparation. For N−Ac-glycine, 100 μL of labeled compound was added to 20 μL of D_2O + 240 μL of DMSO-d_6 + 40 μL of H_2O + 1.7 mg of TEMPOL producing 400 μL of 44 mM sample and 25 mM radical in 60:30:10 DMSO-d_6:D_2O:H_2O (v:v:v). For N−Ac-6-amino-2-naphthoic acid, 100 μL of the labeled compound was added to 120 μL of D_2O + 140 μL of DMSO-d_6 + 40 μL of H_2O + 1.7 mg of TEMPOL producing 400 μL of 44 mM sample and 25 mM radical in 60:30:10 DMSO-d_6:D_2O:H_2O (v:v:v). For the mixture of the 2 compounds, 100 μL of each labeled molecule was added to 20 μL of D_2O + 140 μL of DMSO-d_6 + 40 μL of H_2O + 1.7 mg of TEMPOL producing 400 μL of 44 mM of each compound and 25 mM radical in 60:30:10 DMSO-d_6:D_2O:H_2O (v:v:v).

NMR Experiments. NMR samples for STD experiments consisted of a 2 mM fragment in 0.5:10:89.5 DMSO-d_6:D_2O:phosphate buffer pH 8.5 (v:v:v) together with a protein concentration of 5 μm for HSA. Standard 1D, STD, NMR spectra were acquired at 20 °C with an Avance III HD Bruker Biospin 600 MHz NMR spectrometer (14.1 T), equipped with a 5 mm triple-resonance inverse cryoprobe with a z-axis field gradient. NMR experiments were performed at 298 K with excitation sculpting to suppress peaks from water. 1D and STD NMR experiments were performed using 16 and 512 scans, respectively, with 2 s of recycling delay and 2 s of acquisition time. Specific parameters for the STD experiments (saturation frequency and saturation time) were identical for both samples. Selective saturation of the protein NMR spectrum was achieved with the decoupler offset at 0.7 ppm, and nonsaturation control was performed at −50 ppm. The saturation time was set to 2 s for all experiments with 2 s of recycling delay, 2 s of acquisition time, and 512 scans.

44 mM of the sample was mixed with 25 mM TEMPOL in 60:30:10 DMSO-d_6:D_2O:H_2O (v:v:v). For each experiment, 100 μL of the sample was placed in a PEEK sample cup, which was then immersed in the liquid helium bath of the cryostat of our DNP polarizer. The rapid insertion of the sample into the cryostat ensures the formation of a glassy frozen sample. All low-temperature DNP experiments were performed with a prototype DNP polarizer developed by Bruker Biospin operating at variable temperatures of $1.2 \leq T \leq 4.2$ K in a magnetic field B_0 = 7.05 T.

^{1}H and ^{13}C DNP Experiments. DNP was performed by shining frequency-modulated microwave irradiation at 197.648 GHz ± 144 MHz, with a modulation frequency of 500 Hz, onto the sample. Cross-polarization (CP) was used to transfer hyperpolarization from ^{1}H to ^{13}C nuclear spins using a protocol detailed elsewhere.[18,19] Four 6.5 ms CP contacts were performed with a 10 min interval to allow enough time for the protons to repolarize between CP contacts (40 min total time).

https://doi.org/10.1021/acsomega.4c05101
ACS Omega 2025, 10, 3332−3337

Dissolution, Transfer, and Injection Experiments. A solenoid of 1.5 m length was wound around the transfer capillary and fed with a current of 2.5 A, thus generating a 4 mT field along the transfer line. Once maximum polarization was reached, 7 mL of D_2O was pressurized at 6 bar and heated up until it reached a pressure of 9 bar (~180 °C). This hot and pressurized solvent was rapidly transferred to the sample space, achieving sample melting and fast transfer to a homemade prototype NMR injector directly placed in the Bruker Biospin Fourier 80 benchtop NMR spectrometer where 40 μL of 400 mM deuterated-phosphate buffer pH 8.5 was waiting in the NMR tube for experiments without protein. For experiments with protein, 40 μL of 550 μM of HSA in 400 mM deuterated-phosphate buffer pH 8.5 was waiting in the NMR tube such that the final concentration was 40 μM after dissolution (550 μL final volume).

Hyperpolarized Liquid-State NMR Measurements. Hyperpolarized liquid-state NMR spectra were measured by using a Bruker Biospin Fourier 80 benchtop spectrometer (^{1}H nuclear Larmor frequency = 80.222 MHz and ^{13}C nuclear Larmor frequency = 20.172 MHz). After injection, ^{13}C NMR signals were recorded every 5 s for Ac-L30 and 2.5 s for Ac-L08 with a 15° pulse flip angle. Final hyperpolarization enhancements and final concentrations were calculated by cross-calibration with a highly concentrated reference sample. All experimental data were processed in Matlab.

■ ASSOCIATED CONTENT

Data Availability Statement

The experimental data presented in this work can be downloaded from Zenodo 10.5281/zenodo.10995066.

Supporting Information

The Supporting Information is available free of charge at https://pubs.acs.org/doi/10.1021/acsomega.4c05101.

Nuclear spin−lattice relaxation times (T_1) measurements (PDF)

Accession Codes

The MATLAB codes used to analyze the data can be downloaded from Zenodo 10.5281/zenodo.10995062.

■ AUTHOR INFORMATION

Corresponding Author

Sami Jannin − *Universite Claude Bernard Lyon 1, CRMN UMR-5082, CNRS, ENS Lyon, Villeurbanne 69100, France;* orcid.org/0000-0002-8877-4929; Email: sami.jannin@univ-lyon1.fr

Authors

Olivier Cala − *Universite Claude Bernard Lyon 1, CRMN UMR-5082, CNRS, ENS Lyon, Villeurbanne 69100, France;* orcid.org/0000-0003-3579-0973

Charlotte Bocquelet − *Universite Claude Bernard Lyon 1, CRMN UMR-5082, CNRS, ENS Lyon, Villeurbanne 69100, France*

Chloé Gioiosa − *Universite Claude Bernard Lyon 1, CRMN UMR-5082, CNRS, ENS Lyon, Villeurbanne 69100, France; TotalEnergies OneTech, Centre de recherche de Solaize, 69360 Solaize, France*

Felix Torres − *ETH, CH-8093 Zürich, Switzerland; NexMR GmbH, 8952 Schlieren, Switzerland*

Samuel F. Cousin − *Universite Claude Bernard Lyon 1, CRMN UMR-5082, CNRS, ENS Lyon, Villeurbanne 69100, France; Institut de Chimie Radicalaire (UMR CNRS 7273), Aix-Marseille Université, 13013 Marseille, France;* orcid.org/0000-0002-7021-478X

Sylvie Guibert − *Universite Claude Bernard Lyon 1, CRMN UMR-5082, CNRS, ENS Lyon, Villeurbanne 69100, France*

Morgan Ceillier − *Universite Claude Bernard Lyon 1, CRMN UMR-5082, CNRS, ENS Lyon, Villeurbanne 69100, France*

Venita Busse − *Bruker Switzerland AG, Fällanden 8117, Switzerland*

Frank Decker − *Bruker Biospin GmbH, 76287 Rheinstetten, Germany*

James G. Kempf − *Bruker Biospin Corp., Billerica, Massachusetts 01821, United States*

Stuart J. Elliott − *Universite Claude Bernard Lyon 1, CRMN UMR-5082, CNRS, ENS Lyon, Villeurbanne 69100, France; Molecular Sciences Research Hub, Imperial College London, London W120BZ, U.K.;* orcid.org/0000-0002-8726-0635

Quentin Stern − *Universite Claude Bernard Lyon 1, CRMN UMR-5082, CNRS, ENS Lyon, Villeurbanne 69100, France; Department of Chemistry, Northwestern University, Evanston, Illinois 60208, United States*

Aurélien Bornet − *Universite Claude Bernard Lyon 1, CRMN UMR-5082, CNRS, ENS Lyon, Villeurbanne 69100, France; École Polytechnique Fédérale de Lausanne, Institut des Sciences et Ingénierie Chimiques, 1015 Lausanne, Switzerland*

Complete contact information is available at: https://pubs.acs.org/10.1021/acsomega.4c05101

Notes

The authors declare no competing financial interest.

■ ACKNOWLEDGMENTS

This research was supported by ENS Lyon, the French CNRS, Claude Bernard Lyon 1 University, Bruker Biospin, the European Research Council under the European Union's Horizon 2020 research and innovation program (ERC Grant Agreements No. 714519/HP4all and Marie Skłodowska-Curie Grant Agreement No. 766402/ZULF). The authors gratefully acknowledge Bruker Biospin for providing the prototype dDNP polarizer, and particularly Dmitry Eshchenko, Roberto Melzi, Marc Rossire, and Marco Sacher for scientific and technical support. The authors graciously acknowledge Bruno Knittel for lending assistance with the operation of the Bruker Biospin Fourier 80 benchtop NMR system. The authors additionally acknowledge Catherine Jose and Christophe Pages for use of the ISA Prototype Service, and Stéphane Martinez of the UCBL mechanical workshop for machining parts of the experimental apparatus.

■ REFERENCES

(1) Kirsch, P.; Hartman, A. M.; Hirsch, A. K. H.; Empting, M. Concepts and Core Principles of Fragment-Based Drug Design. *Molecules* **2019**, *24* (23), 4309.

(2) Li, Q. Application of Fragment-Based Drug Discovery to Versatile Targets. *Front. Mol. Biosci.* **2020**, *7*, 180.

(3) Murray, C. W.; Rees, D. C. The Rise of Fragment-Based Drug Discovery. *Nature Chem.* **2009**, *1* (3), 187−192.

(4) Qin, J.; Gronenborn, A. M. Weak Protein Complexes: Challenging to Study but Essential for Life. *FEBS Journal* **2014**, *281* (8), 1948−1949.

(5) *Fragment-Based Drug Discovery and X-Ray Crystallography*; Davies, T. G.; Hyvönen, M., Eds.; Topics in Current Chemistry; Springer Berlin Heidelberg: Berlin, Heidelberg, 2012; Vol. *317*.
(6) Pellecchia, M.; Sem, D. S.; Wüthrich, K. Nmr in Drug Discovery. *Nat. Rev. Drug Discov* **2002**, *1* (3), 211−219.
(7) Fernández, C.; Jahnke, W. New Approaches for NMR Screening in Drug Discovery. *Drug Discovery Today: Technologies* **2004**, *1* (3), 277−283.
(8) Aguirre, C.; Cala, O.; Krimm, I. Overview of Probing Protein-Ligand Interactions Using NMR. *Curr. Protoc. Protein Sci.* **2015**, *81* (1), 17.18.1.
(9) Cala, O.; Krimm, I. Ligand-Orientation Based Fragment Selection in STD NMR Screening. *J. Med. Chem.* **2015**, *58* (21), 8739−8742.
(10) Cala, O.; Guillière, F.; Krimm, I. NMR-Based Analysis of Protein−Ligand Interactions. *Anal Bioanal Chem.* **2014**, *406* (4), 943−956.
(11) Ardenkjaer-Larsen, J. H. Hyperpolarized MR−What's up Doc? *J. Magn. Reson.* **2019**, *306*, 124−127.
(12) Lee, Y.; Zeng, H.; Ruedisser, S.; Gossert, A. D.; Hilty, C. Nuclear Magnetic Resonance of Hyperpolarized Fluorine for Characterization of Protein−Ligand Interactions. *J. Am. Chem. Soc.* **2012**, *134* (42), 17448−17451.
(13) Lerche, M. H.; Meier, S.; Jensen, P. R.; Baumann, H.; Petersen, B. O.; Karlsson, M.; Duus, J. Ø.; Ardenkjær-Larsen, J. H. Study of Molecular Interactions with 13C DNP-NMR. *J. Magn. Reson.* **2010**, *203* (1), 52−56.
(14) Kress, T.; Walrant, A.; Bodenhausen, G.; Kurzbach, D. Long-Lived States in Hyperpolarized Deuterated Methyl Groups Reveal Weak Binding of Small Molecules to Proteins. *J. Phys. Chem. Lett.* **2019**, *10* (7), 1523−1529.
(15) Stern, Q.; Milani, J.; Vuichoud, B.; Bornet, A.; Gossert, A. D.; Bodenhausen, G.; Jannin, S. Hyperpolarized Water to Study Protein−Ligand Interactions. *J. Phys. Chem. Lett.* **2015**, *6* (9), 1674−1678.
(16) Shanaiah, N.; Desilva, M. A.; Nagana Gowda, G. A.; Raftery, M. A.; Hainline, B. E.; Raftery, D. Class Selection of Amino Acid Metabolites in Body Fluids Using Chemical Derivatization and Their Enhanced ^{13} C NMR. *Proc. Natl. Acad. Sci. U.S.A.* **2007**, *104* (28), 11540−11544.
(17) Torres, F.; Bütikofer, M.; Stadler, G. R.; Renn, A.; Kadavath, H.; Bobrovs, R.; Jaudzems, K.; Riek, R. Ultrafast Fragment Screening Using Photo-Hyperpolarized (CIDNP) NMR. *J. Am. Chem. Soc.* **2023**, *145* (22), 12066−12080.
(18) Elliott, S. J.; Stern, Q.; Ceillier, M.; El Daraï, T.; Cousin, S. F.; Cala, O.; Jannin, S. Practical Dissolution Dynamic Nuclear Polarization. *Prog. Nucl. Magn. Reson. Spectrosc.* **2021**, *126−127*, 59−100.
(19) Elliott, S. J.; Ceillier, M.; Cala, O.; Stern, Q.; Cousin, S. F.; Jannin, S. Simple and Cost-Effective Cross-Polarization Experiments under Dissolution-Dynamic Nuclear Polarization Conditions with a 3D-Printed 1H-13C Background-Free Radiofrequency Coil. *J. Magn. Reson. Open* **2022**, *10−11*, No. 100033.
(20) Bornet, A.; Pinon, A.; Jhajharia, A.; Baudin, M.; Ji, X.; Emsley, L.; Bodenhausen, G.; Ardenkjaer-Larsen, J. H.; Jannin, S. Microwave-Gated Dynamic Nuclear Polarization. *Phys. Chem. Chem. Phys.* **2016**, *18* (44), 30530−30535.
(21) Bornet, A.; Milani, J.; Vuichoud, B.; Perez Linde, A. J.; Bodenhausen, G.; Jannin, S. Microwave Frequency Modulation to Enhance Dissolution Dynamic Nuclear Polarization. *Chem. Phys. Lett.* **2014**, *602*, 63−67.
(22) Jannin, S.; Bornet, A.; Melzi, R.; Bodenhausen, G. High Field Dynamic Nuclear Polarization at 6.7T: Carbon-13 Polarization above 70% within 20min. *Chem. Phys. Lett.* **2012**, *549*, 99−102.
(23) Ceillier, M.; Cala, O.; El Daraï, T.; Cousin, S. F.; Stern, Q.; Guibert, S.; Elliott, S. J.; Bornet, A.; Vuichoud, B.; Milani, J.; Pages, C.; Eshchenko, D.; Kempf, J. G.; Jose, C.; Lambert, S. A.; Jannin, S. An Automated System for Fast Transfer and Injection of Hyperpolarized Solutions. *J. Magn. Reson. Open* **2021**, *8−9*, No. 100017.
(24) Milani, J.; Vuichoud, B.; Bornet, A.; Miéville, P.; Mottier, R.; Jannin, S.; Bodenhausen, G. A Magnetic Tunnel to Shelter Hyperpolarized Fluids. *Rev. Sci. Instrum.* **2015**, *86* (2), No. 024101.
(25) Dey, A.; Charrier, B.; Martineau, E.; Deborde, C.; Gandriau, E.; Moing, A.; Jacob, D.; Eshchenko, D.; Schnell, M.; Melzi, R.; Kurzbach, D.; Ceillier, M.; Chappuis, Q.; Cousin, S. F.; Kempf, J. G.; Jannin, S.; Dumez, J.-N.; Giraudeau, P. Hyperpolarized NMR Metabolomics at Natural ^{13} C Abundance. *Anal. Chem.* **2020**, *92* (22), 14867−14871.
(26) Bornet, A.; Maucourt, M.; Deborde, C.; Jacob, D.; Milani, J.; Vuichoud, B.; Ji, X.; Dumez, J.-N.; Moing, A.; Bodenhausen, G.; Jannin, S.; Giraudeau, P. Highly Repeatable Dissolution Dynamic Nuclear Polarization for Heteronuclear NMR Metabolomics. *Anal. Chem.* **2016**, *88* (12), 6179−6183.
(27) Dumez, J.-N.; Milani, J.; Vuichoud, B.; Bornet, A.; Lalande-Martin, J.; Tea, I.; Yon, M.; Maucourt, M.; Deborde, C.; Moing, A.; Frydman, L.; Bodenhausen, G.; Jannin, S.; Giraudeau, P. Hyperpolarized NMR of Plant and Cancer Cell Extracts at Natural Abundance. *Analyst* **2015**, *140* (17), 5860−5863.
(28) Katsikis, S.; Marin-Montesinos, I.; Ludwig, C.; Günther, U. L. Detecting Acetylated Aminoacids in Blood Serum Using Hyperpolarized 13C-1H-2D-NMR. *J. Magn. Reson.* **2019**, *305*, 175−179.
(29) Wilson, D. M.; Hurd, R. E.; Keshari, K.; Van Criekinge, M.; Chen, A. P.; Nelson, S. J.; Vigneron, D. B.; Kurhanewicz, J. Generation of Hyperpolarized Substrates by Secondary Labeling with [1,1- ^{13} C] Acetic Anhydride. *Proc. Natl. Acad. Sci. U.S.A.* **2009**, *106* (14), 5503−5507.
(30) Campos-Olivas, R. NMR Screening and Hit Validation in Fragment Based Drug Discovery. *CTMC* **2011**, *11* (1), 43−67.
(31) Dalvit, C.; Flocco, M.; Knapp, S.; Mostardini, M.; Perego, R.; Stockman, B. J.; Veronesi, M.; Varasi, M. High-Throughput NMR-Based Screening with Competition Binding Experiments. *J. Am. Chem. Soc.* **2002**, *124* (26), 7702−7709.
(32) Ditzler, R. A. J.; Zhukhovitskiy, A. V. Sigmatropic Rearrangements of Polymer Backbones: Vinyl Polymers from Polyesters in One Step. *J. Am. Chem. Soc.* **2021**, *143* (48), 20326−20331.
(33) Dherange, B. D.; Kelly, P. Q.; Liles, J. P.; Sigman, M. S.; Levin, M. D. Carbon Atom Insertion into Pyrroles and Indoles Promoted by Chlorodiazirines. *J. Am. Chem. Soc.* **2021**, *143* (30), 11337−11344.
(34) Milani, J.; Vuichoud, B.; Bornet, A.; Melzi, R.; Jannin, S.; Bodenhausen, G. Hyperpolarization of Nitrogen-15 Nuclei by Cross Polarization and Dissolution Dynamic Nuclear Polarization. *Rev. Sci. Instrum.* **2017**, *88* (1), No. 015109.
(35) Zhang, C.; Xu, L.; Huang, Q.; Wang, Y.; Tang, H. Detecting Submicromolar Analytes in Mixtures with a 5 min Acquisition on 600 MHz NMR Spectrometers. *J. Am. Chem. Soc.* **2023**, *145* (47), 25513−25517.
(36) Reisenbauer, J. C.; Green, O.; Franchino, A.; Finkelstein, P.; Morandi, B. Late-Stage Diversification of Indole Skeletons through Nitrogen Atom Insertion. *Science* **2022**, *377* (6610), 1104−1109.
(37) Woo, J.; Stein, C.; Christian, A. H.; Levin, M. D. Carbon-to-Nitrogen Single-Atom Transmutation of Azaarenes. *Nature* **2023**, *623* (7985), 77−82.

https://doi.org/10.1021/acsomega.4c05101
ACS Omega 2025, 10, 3332−3337